ИЗВЕСТИЯ ВЫСШИХ УЧЕБНЫХ ЗАВЕДЕНИЙ.
Т 68 (1) Серия «**ХИМИЯ И ХИМИЧЕСКАЯ ТЕХНОЛОГИЯ**» 2025

V 68 (1) **ChemChemTech** 2025

DOI: 10.6060/ivkkt.20256801.7085

УДК: 546.02; 546.05

ФАЗООБРАЗОВАНИЕ И СВОЙСТВА ФЕРРОТИТАНАТОВ ВИСМУТА ПРИ ЗАМЕЩЕНИИ ИОНАМИ ТЯЖЕЛЫХ ЛАНТАНОИДОВ (Tb, Er, Ho, Yb)

А.В. Митрофанова, Е.А. Фортальнова, М.Г. Сафроненко, Е.Д. Политова, А.В. Мосунов

Анна Владимировна Митрофанова (ORCID 0000-0003-1207-5512)*, Елена Александровна Фортальнова (ORCID 0000-0002-8120-4376), Марина Геннадьевна Сафроненко (ORCID 0000-0001-8919-622X)

Кафедра общей и неорганической химии, Факультет физико-математических и естественных наук, Российский университет дружбы народов, ул. Миклухо-Маклая, 6, Москва, Российская Федерация, 117198
E-mail: chemistann@gmail.com*, fortalnova_ea@rudn.ru, safronenko_mg@rudn.ru

Екатерина Дмитриевна Политова (ORCID 0000-0002-4158-6314)

Лаборатория функциональных нанокомпозитов, Федеральный исследовательский центр химической физики им. Н.Н. Семенова РАН, ул. Косыгина, 4, Москва, Российская Федерация, 119991
E-mail: politova@nifhi.ru

Александр Викторович Мосунов (ORCID 0000-0002-8904-9593)

Лаборатории технологии функциональных материалов, Кафедра химической технологии и новых материалов, Московский государственный университет им. М.В. Ломоносова, ул. Ленинские горы, 1, Москва, Российская Федерация, 119991
E-mail: mosunov@mail.ru

Цель данного исследования состояла в изучении влияния катионных замещений на формирование фаз Ауривиллиуса при различных температурах термообработки в условиях твердофазного синтеза. Изучено фазообразование ферротитанатов висмута лантаноида со структурой фаз Ауривиллиуса состава $Ln_2Bi_3FeTi_3O_{15}$, где Ln = Tb, Ho, Er, Yb. Полученные образцы охарактеризованы методами рентгеновской дифракции, инфракрасной спектроскопии, дифференциально-термического и термогравиметрического анализа, кроме того, изучен их элементный состав. В выбранном режиме синтеза выявленно преимущественное формирование фазы со структурой пирохлора во всем изученном ряду, за исключением образца, содержащего катионы иттербия(III), в котором сосуществуют фазы пирохлорного типа и слоистого перовскита со структурой Ауривиллиуса. Основная во всех образцах фаза пирохлорного типа кристаллизуется в кубической сингонии. Показано, что в образцах $Ln_2Bi_3FeTi_3O_{15}$, где Ln = Tb, Ho, Er параметры кристаллической решетки уменьшаются, ввиду снижения катионного радиуса ионов Ln(III). Однако в последнем образце изученного ряда $Yb_2Bi_3FeTi_3O_{15}$ данная закономерность нарушается ввиду распределения ионов Yb(III) между фазами перовскита и пирохлора. Установлено, что проявляющиеся в образцах $Ln_2Bi_3FeTi_3O_{15}$, где Ln = Tb, Ho, Er, обратимые термоэффекты могут быть отнесены к фазовому переходу типа порядок-беспорядок в пирохлорной структуре. При изучении температурного поведения двухфазного образца $Yb_2Bi_3FeTi_3O_{15}$ выявлены два обратимых фазовых перехода: термоэффект с низкой интенсивностью характеризует изменения в структуре пирохлорного типа, а более интенсивный термоэффект можно отнести к сегнетоэлектрическому фазовому переходу в структуре слоистого перовскита семейства Ауривиллиуса.

Ключевые слова: фазообразование, структура пирохлора, фаза Ауривиллиуса, фазовые переходы

Для цитирования:
Митрофанова А.В., Фортальнова Е.А., Сафроненко М.Г., Политова Е.Д., Мосунов А.В. Фазообразование и свойства ферротитанатов висмута при замещении ионами тяжелых лантаноидов (Tb, Er, Ho, Yb). *Изв. вузов. Химия и хим. технология*. 2025. Т. 68. Вып. 1. С. 48–54. DOI: 10.6060/ivkkt.20256801.7085.

For citation:
Mitrofanova A.V., Fortalnova E.A., Safronenko M.G., Politova E.D., Mosunov A.V. Phase formation and properties of bismuth ferrotitanates substituted by heavy lanthanide ions (Tb, Er, Ho, Yb). *ChemChemTech [Izv. Vyssh. Uchebn. Zaved. Khim. Khim. Tekhnol.]*. 2025. V. 68. N 1. P. 48–54. DOI: 10.6060/ivkkt.20256801.7085.

PHASE FORMATION AND PROPERTIES OF BISMUTH FERROTITANATES SUBSTITUTED BY HEAVY LANTHANIDE IONS (Tb, Er, Ho, Yb)

A.V. Mitrofanova, E.A. Fortalnova, M.G. Safronenko, E.D. Politova, A.V. Mosunov

Anna V. Mitrofanova (ORCID 0000-0003-1207-5512)*, Elena A. Fortalnova (ORCID 0000-0002-8120-4376), Marina G. Safronenko (ORCID 0000-0001-8919-622X)

Department of General and Inorganic Chemistry, Faculty of Physical, Mathematical and Natural Sciences, RUDN University, Miklukho-Maklaya st., 6, Moscow, 117198, Russia
E-mail: chemistann@gmail.com*, fortalnova_ea@rudn.ru, safronenko_mg@rudn.ru

Ekaterina D. Politova (ORCID 0000-0002-4158-6314)

Laboratory of Functional Nanocomposites, N.N. Semenov Federal Research Center for Chemical Physics of the RAS, Kosygina st., 4, Moscow, 119991, Russia
E-mail: politova@nifhi.ru

Alexandr V. Mosunov (ORCID 0000-0002-8904-9593)

Laboratory of Functional Materials Technology, Department of Chemical Technology and New Materials, Faculty of Chemistry, M.V. Lomonosov Moscow State University, Leninskie Gory, 1, Moscow, 119991, Russia
E-mail: mosunov@mail.ru

The purpose of this study was to investigate the effect of cation substitutions on the formation of Aurivillius phases at various annealing temperatures using solid-state synthesis. The phase formation of lanthanide bismuth ferrotitanates with the Aurivillius phase structure $Ln_2Bi_3FeTi_3O_{15}$, where Ln = Tb, Ho, Er, Yb, has been studied. The obtained samples were characterized by X-ray diffraction, infrared spectroscopy, differential thermal and thermogravimetric analysis, and their elemental composition was studied. The predominant formation of a phase with a pyrochlore structure was revealed in the entire series studied in the chosen synthesis conditions. The exception was the sample containing ytterbium(III) cations, in which phases of the pyrochlore type and layered perovskite with the Aurivillius structure coexist. The main pyrochlore-type phase in all samples crystallizes in the cubic syngony. It is shown that in the $Ln_2Bi_3FeTi_3O_{15}$ samples, where Ln = Tb, Ho, Er, the crystal lattice parameters decrease due to a decrease in the cationic radius of the Ln(III) ions. However, in the last sample of the studied series $Yb_2Bi_3FeTi_3O_{15}$, this pattern is violated because of Yb(III) ions distribution between the perovskite and pyrochlore phases. It has been established that the thermal effects observed in the samples $Ln_2Bi_3FeTi_3O_{15}$, where Ln = Tb, Ho, Er, can be attributed to an order-disorder phase transition in the pyrochlore structure. When studying the temperature behavior of a two-phase sample of $Yb_2Bi_3FeTi_3O_{15}$, two reversible phase transitions were revealed: a low-intensity thermal effect characterizes changes in the pyrochlore-type structure, and a more intense thermal effect can be attributed to a ferroelectric phase transition in the structure of a layered perovskite of the Aurivillius family.

Keywords: phase formation, pyrochlore structure, Aurivillius phase, phase transitions

INTRODUCTION

Currently, ferroelectrics are a large group of popular functional materials. Ferroelectric oxide ceramics can be applied in many devices such as sensors, optical processors, filters, resonators, multilayer capacitors, converters, LEDs, microelectromechanical systems, and memory devices [1, 2].

The environmental side of the issue is also becoming an urgent task for researchers. At some stage of the development of ferroelectricity, most devices were made from lead-containing ceramics, such as lead

zirconate titanate and its solid solutions, due to their high performance. However, waste from the use of these compounds can cause serious environmental problems. Therefore, currently there is an increasing necessity to develop lead-free ferroelectric ceramics to minimize environmental pollution [3]. Perovskite-like, layered and pyrochlore phases can become the basis for such materials due to the stability of the structure and extensive possibilities for modification [2, 4-20].

Aurivillius phases have a layered structure consisting of alternating charged layers $[Bi_2O_2]^{2+}$ and perovskite-like blocks containing *m* quantity of layers $[A_{m-1}B_mO_{3m+1}]^{2-}$ [21].

$Bi_5FeTi_3O_{15}$ belongs to the Aurivillius phases with $m = 4$, which have an orthorhombic type of unit cell distortion. It is known that one of the options to modify the composition of $Bi_5FeTi_3O_{15}$ to improve the electrical characteristics and magnetic properties is the substitution of rare earth cations in the bismuth position, due to the proximity of the cation radii of Bi^{3+} and Ln^{3+}. Analysis of known literature sources, as well as the results of our previous studies, allow us to identify the following trends in the sequence of lanthanides La–Pr–Nd–Sm–Gd–Dy. In this sequence, the ionic radius of rare earth elements decreases, and therefore the volume of the unit cell of the resulting phases based on $Bi_5FeTi_3O_{15}$ decreases. The temperature of electrical disorder also tends to decrease [4, 5, 8, 13, 15, 28]. It is necessary to lower this temperature due to the application requirements of devices using these compounds. We assume that the introduction of heavy lanthanides will also continue this trend. Tb, Er, Ho and Yb were chosen in this study due to the lack of information on their influence on the properties of $Bi_5FeTi_3O_{15}$. Numerous publications report that rare earth cations, partially replacing bismuth cations, do not disrupt the layered perovskite-like structure of the $Bi_5FeTi_3O_{15}$ phase. However, an improvement in ferroelectric properties is observed only at a certain concentration of dopants. An excess of rare earth ions suppresses these properties [4-10, 12, 14, 19].

The structure of pyrochlore with the general formula $A_2B_2O_7$ has a cubic unit cell and consists of two interpenetrating sublattices: A_2O with a tetrahedral environment $[OA_4]$ and B_2O_6, consisting of octahedra $[BO_6]$. The range of properties of pyrochlores that are interesting to study includes piezoelectricity, ferromagnetism, ionic conductivity, and the ability to be active in photocatalysis. Similar to perovskites, to vary the composition of these compounds without disturbing the structural type of pyrochlore, various dopants are used due to the "flexibility" of the crystal lattice [12, 22-24].

In numerous articles on the properties of doped $Bi_5FeTi_3O_{15}$ and $Bi_2Ti_2O_7$, researchers pay more attention to the magnetic properties of the resulting compounds [1, 4, 8-9, 12, 25, 26]. Thus, information on the effect of cation substitutions on the electrical properties of these phases is of interest for studying and establishing correlations between composition and properties. The purpose of this work was to identify the direction of phase formation and possibility of obtaining compounds with a layered perovskite structure of the $Ln_2Bi_3FeTi_3O_{15}$ composition as well as to study their electrical properties.

EXPERIMENTAL PART

The objects of study $Ln_2Bi_3FeTi_3O_{15}$ (Ln=Tb, Ho, Er, Yb) (LnBFT) were obtained from extra pure oxides of bismuth(III), iron(III), titanium(IV) and oxides of the corresponding lanthanides Ln(III), taken in stoichiometric quantities.

The following research methods were used to characterize the properties of the obtained compounds. The phase composition of LnBFT samples was determined using X-ray phase analysis (XRD: DRON-7, $\lambda CuK\alpha = 1.54056$ Å), and the crystal lattice parameters were refined using standard software. IR spectroscopic analysis (Nicolet 6700, 4000-50 cm^{-1}, ATR (Pike), diamond) was used to confirm the XRD data on the structure and symmetry of the synthesized compounds. The method of differential thermal and thermogravimetric analysis (DTA/TG: TA Instruments SDT Q–600, ΔT = = 293-1373 K, $\upsilon = 10$ deg/min) was used to study the process of interaction of initial compounds and changes occurring in the resulting samples. The elemental composition of the samples was analyzed using a DFS-8 spectrograph and a MORS-6 spectra recorder (graphite electrodes, direct current I = 15 A, sample weight 50 mg). To study the electrical characteristics of ceramics, the dielectric spectroscopy method was used (HP 4284A, ΔT = 300 – 1300 K, f = 100 Hz – 1 MHz (1 V), Ag electrodes).

The annealing temperature regime was chosen based on literature data and DTA/TG results of the initial stoichiometric mixtures. A number of thermal effects appear on the DTA curves of unannealed mixtures of all samples, which suggests that the interaction process is multistage with the formation of various intermediate phases. In order to study phase formation for the synthesis of $Ln_2Bi_3FeTi_3O_{15}$, the following heat treatment temperatures were chosen: T_1 = 1073 K, T_2 = 1173 K, T_3 = 1273 K, T_4 = 1373 K. Annealing was carried out in a muffle furnace for 6 h at each stage of

the synthesis. Between stages, the mixtures were re-mixed with ethanol for better homogenization and formed in tablets 1cm diameter and 2mm thickness.

RESULTS AND DISCUSSION

X-ray phase analysis (XRD)

According to XRD results all LnBFT samples are multiphase after two synthesis stages T_1 = 1073 K and T_2 = 1173 K. The samples contain the following phases: $Bi_5FeTi_3O_{15}$, $BiFeO_3$, $Bi_2Fe_4O_9$, $Bi_{12}TiO_{20}$.

With an increase in the heat treatment temperature T_3 = 1273 K in the diffraction patterns of the obtained LnBFT samples (Ln = Tb, Er) the most intense reflections belong to the pyrochlore phase $Bi_2Ti_2O_7$, and the reflections of the Aurivillius phase $Bi_5FeTi_3O_{15}$ have low intensity, i.e. this phase is present in listed above samples only in trace amounts (Fig. 1a). In LnBFT samples containing holmium Ho^{3+} and ytterbium Yb^{3+} cations the Aurivillius phase is the main but not the single.

Further annealing at T_4 = 1373 K leads to the completion of phase formation in the sample containing Er^{3+} cations. The diffraction pattern shows only reflections that belong to the pyrochlore phase (Fig. 1b). The remaining samples of the studied series are two-phase and, in addition to the main phase with the pyrochlore structure, contain a trace amounts of Aurivillius phase in case of samples with Tb^{3+} and Ho^{3+}, and more significant quantity in case of YbBFT sample.

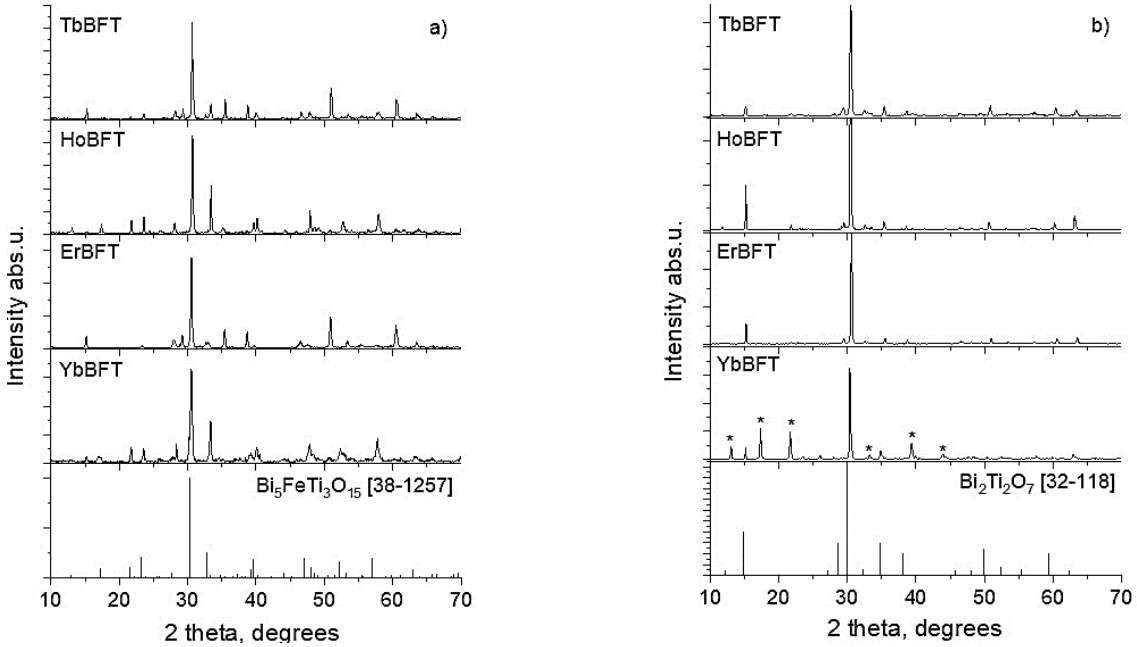

Fig. 1. Diffraction patterns of LnBFT after annealing at: a) T_3=1272 K, b) T_4=1373 K (* – Aurivillius phase)

Рис. 1. Дифрактограммы образцов LnBFT после обжига при: a) T_3=1272 K, b) T_4=1373 K (* – фаза Ауривиллиуса)

According to emission analysis data for samples of the entire LnBFT series after all synthesis stages, the intensity of lines related to bismuth(III) cations remains the same. This indicates the absence of significant losses of bismuth(III) oxide during high-temperature synthesis [5].

For the main phase with the pyrochlore type in LnBFT samples, crystallized in a cubic system, the crystal lattice parameters were refined after annealing at T_4 = 1373 K (Table). It has been established that with increasing atomic number Ln = Tb, Ho, Er a linear decrease in the unit cell volume occurs due to a decrease in the radius of the Ln^{3+} because of the f-compression.

However, the unit cell parameters of pyrochlore in YbBFT sample deviate from a linear correlation. In YbBFT, the pyrochlore and layered perovskite phases coexist in almost equal proportions. Presumably, Yb^{3+} ions are distributed unevenly between the two phases, being localized predominantly in the Aurivillius phase.

Table

Unit cell parameters of the pyroclore phase LnBFT T_4 = 1373 K

***Таблица*. Параметры элементарной ячейки фазы со структурой пирохлора образцов LnBFT T_4 = 1373 K**

Cation Ln^{3+}	a, Å	V, Å^3
Tb^{3+}	20,310±0,007	8378±8
Ho^{3+}	20,251±0,007	8304±8
Er^{3+}	20,212±0,006	8257±7
Yb^{3+}	20,417±0,007	8510±8

IR spectroscopy

In the IR spectra of layered perovskites bands characteristic of symmetric and asymmetric stretching vibrations of Me-O bond in MO_6 octahedra appear in the range 900-650 cm^{-1}, while bands related to bending vibrations in octahedra MO_6 and $[Bi_2O_2]^{2+}$ groups occur in the range 650-200 cm^{-1} [27]. A fragment of the pyrochlore crystal structure, similar to the perovskite structure, is the MeO_6 octahedra. Accordingly, absorption bands of Me-O bonds vibrations in MeO_6 of the pyrochlore structure also appear in the range 900-200 cm^{-1}. In addition, a decrease in the number of bands in the IR spectrum indicates an increase in the symmetry of the crystal lattice.

According to the results of IR spectroscopic analysis of LnBFT samples after T_3 = 1273 K, in the spectra of HoBFT and YbBFT containing the Aurivillius phase as the main phase two absorption bands appear in the frequency range 900-550 cm^{-1}, characteristic of stretching vibrations of the Me-O bond (Me = = Ti(IV), Fe(III)) in MeO_6 octahedra of the crystal structure. The presence of a shoulder on the high-frequency slope of the 750-550 cm^{-1} band indicates an orthorhombic distortion of the unit cell. A decrease in the intensity of the band in the range 900-750 cm^{-1} for TbBFT and ErBFT indicates a decrease in the content of the perovskite-like phase in the sample, which is consistent with the results of diffraction studies.

After annealing at T_4 = 1373 K, the IR spectra of all samples of the studied series contain a band in the range 750-550 cm^{-1}. Based on the XRD results, it was established that in LnBFT (Ln = Tb, Er, Ho) after T_4 = 1373 K the main phase is the pyrochlore phase, and the layered perovskite phase is contained in trace amounts. In the IR spectra of LnBFT (Ln = Tb, Er, Ho) the absorption band in the range 900-750 cm^{-1} has low intensity or almost absent. Unlike the other studied samples of the series, YbBFT contains a significant amount of the Aurivillius phase, which is reflected in the IR-spectrum by the appearance of two absorption bands in the range 900-550 cm^{-1}.

Differential thermal analysis (DTA)

The results of studies of the temperature behavior of the obtained LnBFT samples after annealing at T_4 = 1373 K are presented in Fig. 2. All DTA curves revealed thermal effects characterizing reversible structural changes.

Thermal effects in LnBFT samples (Ln = Tb, Er, Ho) are diffuse, accompanied by significant hysteresis (~100 K) and can be attributed to an order-disorder phase transition in the structure of pyrochlore [28]. The occurrence of two reversible thermal effects at close temperatures in the DTA curve of HoBFT sample is likely due to the different distribution of substituting Fe(III) and Ho(III) cations in positions A and B of the pyrochlore $A_2B_2O_7$ structure.

The ferroelectric phase transition in the $Bi_5FeTi_3O_{15}$ structure appears at ~1023 K (hysteresis 10 K) [28], however, the replacement of 40% of bismuth positions by Ln(III) ions leads to a significant increase in the temperature of this effect [29]. In YbBFT sample, where the perovskite and pyrochlore phases coexist, two reversible thermal effects appear. The thermal effect, related to changes in the structure of pyrochlore, has low intensity and occurs at a temperature of 1073 K. A ferroelectric phase transition with a higher intensity is observed at 1295 K.

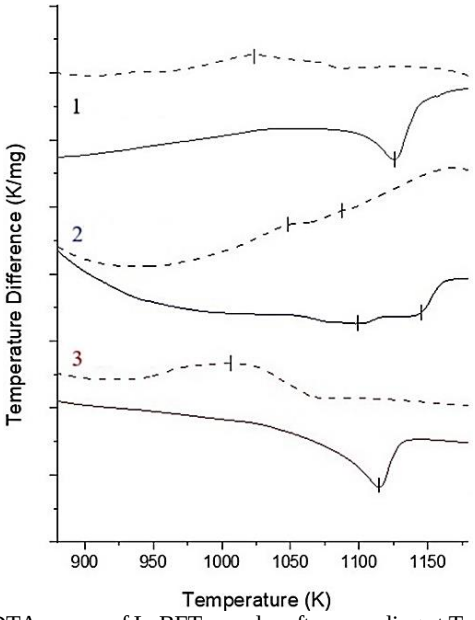

Fig. 2. DTA-curves of LnBFT samples after annealing at T_4=1373 K (solid lines – heating, dotted lines – cooling): 1) TbBFT, 2) HoBFT, 3) ErBFT

Рис. 2. Кривые ДТА образцов LnBFT после обжига при T_4=1373 K (сплошные линии – нагревание, пунктирные линии – охлаждение): 1) TbBFT, 2) HoBFT, 3) ErBFT

Dielectric spectroscopy

DTA data confirm studies of the temperature dependence of dielectric constant. Frequency-dependent and frequency-independent anomalies were revealed in the dielectric constant (ε) curves of the obtained LnBFT samples. Frequency-dependent anomalies relate to relaxation processes in ceramics, while frequency-independent anomalies indicate the temperatures of phase transitions (Fig. 3).

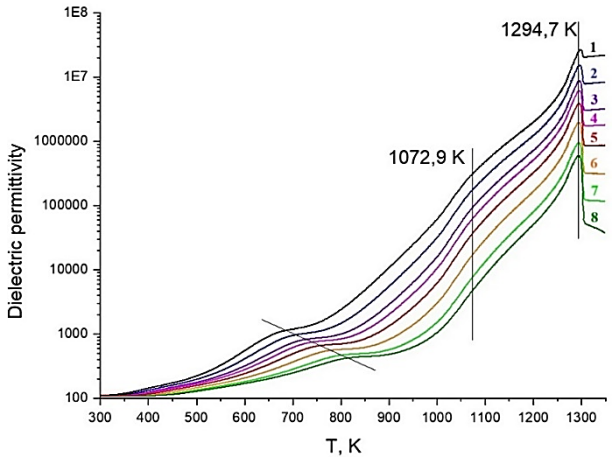

Fig. 3. Temperature dependences of the dielectric constant of YbBFT ε(T) after annealing at T_4 = 1373 K obtained in the cooling mode at frequencies f: 1) 500 Hz, 2) 1 kHz, 3) 2 kHz, 4) 3 kHz, 5) 5 kHz, 6) 10 kHz, 7) 20 kHz, 8) 30 kHz

Рис. 3. Температурные зависимости диэлектрической проницаемости ε(T) образца YbBFT после обжига при T_4 = 1373 K, полученные в режиме охлаждения на частотах f: 1) 500 Гц, 2) 1 кГц, 3) 2 кГц, 4) 3 кГц, 5) 5 кГц, 6) 10 кГц, 7) 20 кГц, 8) 30 кГц

CONCLUSION

It was revealed that heavy lanthanides doping significantly affects the phase formation of bismuth ferrotitanates $Ln_2Bi_3FeTi_3O_{15}$. At 1273 K Aurivillius phase is formed along with the pyrochlore phase. Increasing the annealing temperature (1373K) leads to predominantly formation of pyrochlore phase with structure $Bi_2Ti_2O_7$. It has been established that the temperatures of the phase transitions in the studied samples are strongly influenced by the introduction of a rare earth ion.

FINANCING THE WORK

The study was carried out with financial support from the Russian Foundation for Basic Research (Project No. 21-53-12005).

The authors declare the absence a conflict of interest warranting disclosure in this article.

Исследование выполнено при финансовой поддержке Российского фонда фундаментальных исследований (проект № 21-53-12005).

Авторы заявляют об отсутствии конфликта интересов, требующего раскрытия в данной статье.

REFERENCES
ЛИТЕРАТУРА

1. **Chen G., Bai W., Sun L., Wu J., Ren Q., Xu W., Yang J., Meng X., Tang X., Duan C-G., Chu J.** Processing Optimization and Sintering Time Dependent Magnetic and Optical Behaviors of Aurivillius $Bi_5Ti_3FeO_{15}$ Ceramics. *J. Appl. Phys.* 2013. V. 113. N 3. P. 034901. DOI: 10.1063/1.4775800.
2. **Mao X., Wang W., Chen X., Lu Y.** Multiferroic Properties of Layer-structured $Bi_5Fe_{0.5}Co_{0.5}Ti_3O_{15}$ Ceramics. *Appl. Phys. Lett.* 2009. V. 95. P. 082901. DOI: 10.1063/1.3213344.
3. **Moure A.** Review and Perspectives of Aurivillius Structures as a Lead-free Piezoelectric System. *J. Appl. Sci.* 2018. V. 8. P. 62. DOI: 10.3390/app8010062.
4. **Bai Y., Chen J., Tian R., Zhao S.** Enhanced Multiferroic and Magnetoelectric Properties of Ho, Mn Co-doped $Bi_5Ti_3FeO_{15}$ Films. *Mater. Lett.* 2016. V. 164. P. 618–622. DOI: 10.1016/j.matlet.2015.11.083.
5. **Bobic J.D., Katiliute R.M., Ivanov M.** Dielectric, Ferroelectric and Magnetic Properties of La Doped $Bi_5Ti_3FeO_{15}$ Ceramics. *J. Mater. Sci. - Mater. Electron.* 2016. V. 27. N 3. P. 2448–2454. DOI: 10.1007/s10854-015-4044-6.
6. **Chen X., Lu Z., Huang F., Min J., Li J., Xiao J., Yang F., Zeng X.** Molten Salt Synthesis and Magnetic Anisotropy of Multiferroic $Bi_4NdTi_3Fe_{0.7}Ni_{0.3}O_{15}$ Ceramics. *J. Alloys Compd.* 2017. V. 693. P. 448–453. DOI: 10.1016/j.jallcom.2016.09.214.
7. **Chen C-X.,·Liu Y-K., Zheng R-K.** Magnetic and Ferroelectric Properties of $SmBi_4Fe_{0.5}Co_{0.5}Ti_3O_{15}$ Compounds Prepared with Different Synthesis Methods. *J. Mater. Sci. - Mater. Electron.* 2017. V. 28. N 11. P. 7562–7567. DOI: 10.1007/s10854-017-6446-0.
8. **Gil Novoa O.D., Landínez Téllez D.A., Roa-Rojas J.** Synthesis, Structural, Magnetic and Ferroelectric Characterization of Biferroic $Bi_3R_2FeTi_3O_{15}$. *Rev. Mex. de Fis.* 2012. V. 58. N 2. P. 77–80. DOI: 10.1016/j.physb.2011.12.035.
9. **Peña O., Guizouarn T., Moure C., Gil V., Tartaj J.** Magnetic Properties of Aurivillius Lanthanide-bismuth $(LnFeO_3)_nBi_4Ti_3O_{12}$ (n = 1,2) Layered Titanates. *Bol. Soc. Esp. Ceram. V.* 2008. V. 47. P. 129-132. DOI: 10.3989/cyv.2008.v47.i3.188.
10. **Li J., Pu Y., Wang X., Shi Y., Shi R., Yang M., Wang W., Guo X., Peng X.** Effect of Yttrium Doping on the Structure, Dielectric Multiferroic and Magnetodielectric Properties of $Bi_5Ti_3FeO_{15}$ Ceramics. *J. Mater. Sci. - Mater. Electron.* 2020. V. 31. P. 4345–4353. DOI: 10.1007/s10854-020-02992-w.
11. **Ломанова Н.А., Томкович М.В., Осипов А.В., Уголков В.Л., Панчук В.В., Семенов В.Г.** Формирование и термическое поведение твердых растворов $Bi_{5-x}Ca_xFeTi_3O_{15-\delta}$. *Журн. общей химии.* 2020. Т. 90. № 6. С. 935–940. DOI: 10.31857/S0044460X20060145. **Lomanova N.A., Tomkovich M.V., Osipov A.V., Ugolkov V.L., Panchuk V.V., Semenov V.G.** Synthesis and Thermal Behavior of $Bi_{5-x}Ca_xFeTi_3O_{15-\delta}$ Solid Solutions. *Russ. J. Gen. Chem.* 2020. V. 90. N 6. P. 1025–1029. DOI: 10.1134/S1070363220060146.
12. **Ragsdale W., Gupta S., Conard K., Delacruz S., Subramanian R.V.** Photocatalytic Activity of Fe-modified Bismuth Titanate Pyrochlores: Insights into Its Stability, Photoelectrochemical, and Optical Responses. *Appl. Catal. B.* 2016. V. 180. P. 442-450. DOI: 10.1016/j.apcatb.2015.06.016.
13. **Rehman F., Jin H-B., Niu C., Bukhtiar A., Zhao Y-J., Lin J-B.** Structural, Magnetic and Dielectric Properties of $Bi_4Nd_{0.5}Gd_{0.5}Ti_3FeO_{15}$ Ceramics. *Ceram. Int.* 2016. V. 42. N 2. P. 2806–2812. DOI: 10.1016/j.ceramint.2015.11.013.
14. **Sun H., Niu J., Cheng H., Lu Y., Xu Z., Zhang L., Chen X.** Effects of Ni Substitution on Multiferroic Properties in $Bi_5FeTi_3O_{15}$ Ceramics. *Chin. Phys. B.* 2021. V. 30. N 10. P. 107701. DOI: 10.1088/1674-1056/ac1b92.
15. **Ti R., Huang F., Zhu W., He J., Xu T., Yue C., Zhao J., Lu X., Zhu J.** Multiferroic and Dielectric Properties of $Bi_4LaTi_3FeO_{15}$ Ceramics. *Ceram. Int.* 2015. V. 41. P. 453–457. DOI: 10.1016/j.ceramint.2015.03.157.
16. **Zhao H., Wang H., Cheng Z., Fu Q., Tao H., Ma Z., Jia T., Kimura H., Li H.** Electric and Magnetic Properties of Aurivillius-phase Compounds: $Bi_5Ti_3XO_{15}$ (X = Cu, Mn, Ni, V).

Ceram. Int. 2018. V. 44. N 11. P. 13226-13231. DOI: 10.1016/j.ceramint.2018.04.148.

17. **Zuo X., Hui Z., He E., Zhao G., Bai J., Wu J., Zhu S., Kan X., Song W., Yang J., Zhu X., Dai J.** Effects of W/Ni Co-doping on the Structural, Magnetic, Electrical, and Optical Properties of Aurivillius Phase $Bi_5FeTi_3O_{15}$ Ceramics. *J. Mater. Sci. - Mater. Electron.* 2020. V. 31. P. 11131–11140. DOI: 10.1007/s10854-020-03662-7.
18. **Zuo X., Zhang M., He E., Guan B.** Structural, Magnetic, and Dielectric Properties of W/Cr Co-substituted Aurivillius $Bi_5FeTi_3O_{15}$. *J. Alloys Compd*. 2017. V. 726. P. 1040-1046. DOI: 10.1016/j.jallcom.2017.08.077.
19. **Zuo X.Z., Zhang M.L., He E.J., Yang J., Zhu X.B., Dai J.M.** Multiferroic Property, Dielectric Response, and Scaling Behavior in Aurivillius $Bi_{4.25}Gd_{0.75}Fe_{0.5}Co_{0.5}Ti_3O_{15}$ Ceramic. *J. Alloys Compd*. 2017. V. 695. P. 2556–2562. DOI: 10.1016/j.jallcom.2016.11.161.
20. **Опра Д.П., Синебрюхов С.Л., Неумоин А.И., Подгорбунский А.Б., Гнеденков С.В.** Мезопористые нанотрубчатые материалы на основе $Na_2Ti_3O_7$ с иерархической архитектурой: синтез и свойства. *Изв. вузов. Химия и хим. технология*. 2022. Т. 65. Вып. 12. С. 37-43. **Opra D.P., Sinebryukhov S.L., Neumoin A.I., Podgorbunsky A.B., Gnedenkov S.V.** Mesoporous $Na_2Ti_3O_7$ Nanotube-Constructed Materials with Hierarchical Architecture: Synthesis and Properties. *ChemChemTech [Izv. Vyssh. Uchebn. Zaved. Khim. Khim. Tekhnol.]*. 2022. V. 65. N 12. P. 37-43. DOI: 10.6060/ivkkt.20226512.6552.
21. **Shashkov M.S., Malyshkina O.V., Piir I.V., Koroleva M.S.** Dielectric Properties of Iron Containing Bismuth Titanate Solid Solutions with a Layered Perovskite Structure. *Phys. Solid State.* 2015. V. 57. N 3. P. 518–521. DOI: 10.1134/S1063783415030312.
22. **Mrázek J., Boháček J., Vytykáčová S., Buršík J., Puchý V., Robert D., Kašík I.** Photolithographic Patterning of Nanocrystalline Europium-titanate $Eu_2Ti_2O_7$ Thin Films on Silicon Substrates. *Mater. Lett.* 2017. V. 209. P. 216-219. DOI: 10.1016/j.matlet.2017.08.013.
23. **Ping X., Liu Y., Chen S., Ran N., Zheng L., Wang M., Guo L., Wei Z.** Tailoring B-site of Lead-ruthenate Pyrochlore for Boosting Acidic Water Oxidation Activity and Stability. *Appl. Catal. B.* 2022. V. 318. P. 121884. DOI: 10.1016/j.apcatb.2022.121884.
24. **Мясников Д.А., Потураев П.С., Красновских М.П., Мокрушин И.Г.** Цирконат празеодима: фазообразование при термической обработке и электрохимичексое поведение. *Изв. вузов. Химия и хим. технология.* 2022. Т. 65. Вып. 9. С. 6-12. **Myasnikov D.A., Poturaev P.S., Krasnovskikh M.P., Mokrushin I.G.** Praseodimum Zirconate: Phase Formation During Heat Treatmentand Electrochemicalbehavior. *ChemChemTech [Izv. Vyssh. Uchebn. Zaved. Khim. Khim. Tekhnol.]*. 2022. V. 65. N 9. P. 6-12. DOI: 10.6060/ivkkt.20226509.6510.
25. **Pikula T., Dzik J., Guzdek P., Mitsiuk V.I., Surowiec Z., Panek R., Jartych E.** Magnetic Properties and Magnetoelectric Coupling Enhancement in $Bi_5Ti_3FeO_{15}$ Ceramics. *Ceram. Int.* 2017. V. 43. P. 11442–11449. DOI: 10.1016/j.ceramint.2017.06.008.
26. **Taguchi Y., Tokura Y.** Giant Negative Magnetoresistance in a Metallic Ferromagnet $Sm_2Mo_2O_7$. *Phys. B Cond. Matt.* 2000. V. 284–288 (Part 2). P. 1448-1449. DOI: 10.1016/S0921-4526(99)02687-3.
27. **Zhou Z-Y., Dong X-L., Yan H-X.** Lanthanum Distribution and Dielectric Properties of $Bi_{3-x}La_xTiNbO_9$ Bismuth Layer-structured Ceramics. *Scripta Mater.* 2006. V. 55. P. 791-794. DOI: 10.1016/j.scriptamat.2006.07.014.
28. **Kabirov U.V., Kupriyanov M.F., Chebanova E.V.** Reconstructive phase transitions of oxygen-octahedral structures. *J. Struct. Chem.* 2009. V. 50. N 3. P. 492 – 496 (in Russian). DOI: 10.1007/s10947-009-0070-7.
29. **Mitrofanova A.V., Fortalnova E.A., Safronenko M.G., Politova E.D.** Properties of Lanthanide Containing Aurivillius Phases $Ln_2Bi_3FeTi_3O_{15}$ (Ln = La, Pr, Nd, Sm, Gd). *Ferroelectrics*. 2022. V. 590. N 1. P. 9-16. DOI: 10.1080/00150193.2022.2037934.

Поступила в редакцию 14.03.2024
Принята к опубликованию 14.06.2024

Received 14.03.2024
Accepted 14.06.2024